Rubor, calor, tumor, dolor: objective assessments of inflammation

Voorde, W. ten

CHAPTER VII

COMPREHENSIVE EVALUATION OF MICRONEEDLE-BASED INTRADERMAL ADALIMUMAB DELIVERY VS. SUBCUTANEOUS ADMINISTRATION: RESULTS OF A RANDOMIZED CONTROLLED CLINICAL TRIAL

Published in the British Journal of Clinical Pharmacology, 2021

Wouter ten Voorde[2,3,8,*] , Justin Jacobse[1,2,3,4,*], Anushka Tandon[2], Stefan G Romeijn[3], Hendrika W Grievink[2], Koen van der Maaden[3], Michiel J van Esdonk[2], Dirk Jan A R Moes[5], Floris Loeff[6], Karien Bloem[6], Annick de Vries[6], Theo Rispens[6], Gertjan Wolbink[6], Marieke de Kam[2], Dimitrios Ziagkos[2], Matthijs Moerland[2], Wim Jiskoot[3], Joke Bouwstra[3], Jacobus Burggraaf[2,3], Lenneke Schrier[1,7], Robert Rissmann[2,3,5,**], Rebecca Ten Cate[1,**]
** Shared first authorship, ** Shared last authorship*

1 Department of Pediatric Rheumatology Willem-Alexander Children's Hospital, Leiden University Medical Center, Leiden, NL
2 Centre for Human Drug Research, Leiden, NL
3 Division of BioTherapeutics, Leiden Academic Centre for Drug Research, Leiden University, Leiden, NL
4 Currently also affiliated with department of Pathology, Microbiology and Immunology at Vanderbilt University, Nashville, Tennessee, USA.
5 Department of Clinical Pharmacy & Toxicology, Leiden University Medical Center, Leiden, NL
6 Biologics Lab, Sanquin Diagnostic Services, Amsterdam, NL
7 Currently at Princess Maxima Centre for Pediatric Oncology, Utrecht, NL
8 Leiden University Medical Center, Leiden, NL

ABSTRACT

AIMS To evaluate feasibility of intradermal (i.d.) adalimumab administration using hollow microneedles, and to compare a single i.d. dose of adalimumab using a hollow microneedle with a single subcutaneous (s.c.) dose using a conventional needle.

METHODS In this single-centre double-blind, placebo-controlled, double-dummy clinical trial in 24 healthy adults we compared 40 mg adalimumab (0.4 mL) administered i.d. using a hollow microneedle with a s.c. dose using a conventional needle. Primary parameters were pain, acceptability and local tolerability; secondary parameters safety, pharmacokinetics and immunogenicity. We explored usability of optical coherence tomography, clinical photography, thermal imaging, and laser speckle contrast imaging to evaluate skin reaction after i.d. injections. In vitro protein analysis was performed to assess compatibility of adalimumab with the hollow microneedle device.

RESULTS While feasible and safe, injection pain of i.d. adalimumab was higher compared to s.c. adalimumab (35.4 vs. 7.9 on a 100-point visual analogue scale). Initial absorption rate and relative bioavailability were higher after i.d. adalimumab (time to maximum plasma concentration = 95 h [47–120]; F_{rel} = 129% [6.46%]) compared to s.c. adalimumab (time to maximum plasma concentration = 120 h [96–221]). Anti-adalimumab antibodies were detected in 50% and 83% of the subjects after i.d. and s.c. adalimumab, respectively. We observed statistically significantly more erythema and skin perfusion after i.d. adalimumab, compared to s.c. adalimumab and placebo injections ($P < .0001$). Cytokine secretion after whole blood lipopolysaccharide challenge was comparable between administration routes.

CONCLUSIONS Intradermal injection of adalimumab using hollowing microneedles was perceived as more painful and less accepted than s.c. administration, but yields a higher relative bioavailability with similar safety and pharmacodynamic effects.

INTRODUCTION

Biopharmaceuticals, such as monoclonal antibodies (mAbs), are used in the treatment of many chronic and life-threatening diseases.[1] Degradation and ineffective absorption of mAbs in the gastrointestinal tract, due to molecular size and conditions such as low PH and digestive enzymes, necessitates their parenteral administration. However, in clinical practice, treatments administered using subcutaneous (s.c.) injection of mAbs have been perceived as unpleasant and painful, especially during long-term use in both adults and children.[2] Thus, s.c. administration may jeopardize treatment adherence and a less invasive and less painful method to administer mAbs is warranted.

Intradermal (i.d.) administration of biopharmaceuticals through hollow microneedles is advocated as a substitute for s.c. injection, due to less pain associated with injection of drugs using microneedles,[3] and i.d. administered biopharmaceuticals may show more favourable pharmacokinetics (PK) as compared to s.c. administration.[4,5,6,7] Multiple types of microneedles exist, such as hollow and solid microneedles, and microneedles have different properties in comparison with conventional needles. For instance, the injection of pharmaceutical compounds using hollow microneedles is more superficial, i.e. into the skin (i.d.) rather than beneath the skin (s.c.). Additionally, the diameter of hollow microneedles is smaller than that of conventional hypodermic needles for s.c. injection. An unbiased and systematic approach is warranted to acquire reliable data on pain perception and patient preferences, as these are subjective concepts.[8] Therefore, it is relevant to compare pain, acceptability and local tolerability, as well as PK and pharmacodynamics (PD) between mAbs administered i.d. using a hollow microneedle with s.c. injection using a conventional hypodermic needle. Moreover, when using a new drug–device combination, chemistry, manufacturing and control aspects need consideration.

The commercially available microneedles used in the clinical trial reported in this paper have been used in various clinical studies.[9] Each device consists of 3 hollow microneedles with a length of 600 µm; this device is hereafter referred to as hollow microneedle. Although microneedle vaccine administration has been widely investigated, there are no systematic reports on MAB administration using microneedles in humans. We choose adalimumab (Humira, AbbVie) as model MAB as it is widely used for a variety of auto-immune/auto-inflammatory diseases including juvenile idiopathic arthritis. Adalimumab acts by binding to the proinflammatory cytokine tumour necrosis factor-α (TNFα), hereby preventing its interaction with the TNFα receptor.[10]

To evaluate feasibility of i.d. adalimumab administration using hollow microneedles, we performed a double-blind, double-dummy, randomized

controlled clinical trial in healthy adults, comparing a single i.d. dose of adalimumab using a hollow microneedle with a single s.c. dose using a conventional needle. Our primary aim was to systematically investigate pain, acceptability and local tolerability after i.d. adalimumab administration and to compare this with s.c. administration. Our secondary aim was to evaluate safety, PK, PD and immunogenicity of i.d. adalimumab administration and to compare this with s.c. administration. Moreover, we explored the usability of optical coherence tomography (OCT), clinical photography, thermal imaging and laser speckle contrast imaging (LSCI) in the evaluation of i.d. injections. Lastly, prior to the clinical trial we performed an elaborate in vitro protein analysis to examine whether ejection of adalimumab through a hollow microneedle bore increases particle formation or protein aggregation compared to ejection through a conventional needle. One could envision that during ejection of a protein out of a narrow microneedle, the structure of the protein might be affected. Factors contributing to the immunogenicity of mAbs include protein structure and physical degradation, such as aggregation.[11] The formation of anti-adalimumab antibodies may result in reduced treatment efficacy due to increased drug clearance (CL).[12,13]

Altogether, in this paper we provide a systematic and comprehensive approach to answer the question of whether hollow microneedles can be used safely and effectively to administer a model MAB.

MATERIALS AND METHODS

STUDY DESIGN

This was a single-centre double-blind, placebo-controlled, double-dummy clinical trial with 4 interventions: i.d. adalimumab (40 mg Humira, AbbVie, Maidenhead, Kent, UK), i.d. saline (0.9%), s.c. adalimumab, and s.c. saline. i.d. injections were given using a hollow microneedle (MicronJet600 from Nanopass Technologies Ltd., Ness Ziona, Israel), s.c. injections using a regular needle (Microlance 3 from Becton, Dickinson and Company [BD], Franklin Lakes, NJ, USA); both devices were connected to a syringe (1 mL Luer-Lok, BD). The length of the 3 needles of a MicronJet600 device is 600 µm. Injections were given according to standard operating procedures and the manufacturer's instruction. All subjects received 1 placebo injection and 1 adalimumab injection of 40 mg in 0.4 mL in the right and left upper lateral thigh by the same physician. Given the nature of the study, the physician administering the injection could not be blinded to the method of administration but was blinded to treatment, i.e., adalimumab or placebo. Therefore, this physician was not involved in the assessment of any of the predefined outcomes (evaluator-blinded). The subjects were in a prone position during and in between injections to ensure blinding (subject-blinded). Injections were spaced 5 minutes apart. Prior to administration, the sites of injection were annotated using a surgical marker (Purple Surgical, Shenley, Herts, UK). Subjects were instructed to maintain the marking while at home, and to prevent excessive sun exposure to the injection site to limit possible interference with the exploratory measurements.

PARTICIPANTS

Twenty-four healthy immunocompetent male and female subjects aged 18–45 years with Fitzpatrick skin type I-II (Caucasian) and not smoking more than 10 cigarettes per day were included in the study. The ratio male:female was 1:1. Subject health status was verified during a medical screening consisting of a medical history, physical examination, vital signs, 12-lead electrocardiogram, laboratory analysis of blood and urine, and a Mantoux and/or interferon-γ (IFN-γ) release assay. Subjects with a history of tuberculosis were excluded. Routine safety assessments were performed as described earlier.[14] Total observation time was 70 days.

SAMPLE SIZE AND RANDOMIZATION

Due to the explorative character of this trial, empirical, early clinical phase cohort sizes were used to answer the objectives of the trial. No formal power calculation was performed. A total of 24 subjects were studied (allocation s.c.: i.d. = 1:1): 12 subjects received i.d. adalimumab and s.c. placebo and 12 subjects received s.c. adalimumab and i.d. placebo. The sequence of injection, i.e., s.c. followed by i.d. injection or i.d. injection followed by s.c. injection, was counterbalanced. Randomization was done in 6 blocks of 4, each 4 arms containing 1 of each 4 sequences (adalimumab s.c. followed by placebo i.d.; placebo i.d. followed by adalimumab s.c.; placebo s.c. followed by adalimumab i.d.; adalimumab i.d. followed by placebo s.c.). The randomization code was generated using SAS 9.4 by a study-independent statistician; treatment allocation was only revealed after completion of blind data review and locking of the data. After screening and assessment for suitability, subjects were enrolled in the trial by a physician. Interventions were assigned to subjects by a study-independent statistician.

OUTCOME MEASURES

A subjective evaluation of spill was performed by visual inspection of the injection site, estimating the volume that was not injected as percentage of the intended injection volume: no spill; minor spill: 15% spillage; major spill: 15–50% spillage; critical spill: >50% spillage. Microneedles were inspected post injection for damage using bright field microscopy.

PAIN, ACCEPTABILITY AND LOCAL TOLERABILITY AFTER I.D. AND S.C. ADALIMUMAB ADMINISTRATION

To quantify pain, visual analogue scale (VAS) scores for pain using both a 10-cm VAS and the Dutch Faces Pain Scales Revised (FPSR)[15] were completed by the volunteers at screening for the Mantoux, or saline if no Mantoux was given, at the time of drug administration, and after drug administration. Pain scores were obtained separately for insertion of the needle (insertion pain) and infusion of the formulation (infusion pain). A standardized injection site examination was performed to evaluate injection sites. Pain was graded as (0) absent; (1) present; no limitations in activity of daily living (ADL); (2) present, limitations in age-appropriate instrumental ADL or requires repeated non-narcotic pain reliever; (3) present, limitations in self-care ADL or interferes with sleep or requires repeated narcotic pain reliever. Induration was scored similarly as injection site pain, but with grade (3) instead being 'limitations in self-care ADL or requires systemic treatment'. Tenderness was graded as: (0) absent; (1) mild discomfort with pressure; (2) discomfort with touch; (3) discomfort elicited by clothing or bed sheets. Pruritus was graded as (0) absent; (1) present, but minimally distracting; (2) present, distracting during routine activities; (3) interferes with sleep. Erythema, blister, ulceration, necrosis and ecchymosis were measured if present.

Subject preference for injection was examined using multiple-choice questions. Subjects were asked how they experienced the injections, how they would like to receive a potential future injection and if they feared the injection(s), using the following options: do you prefer the first injection, the second injection or do you not have a preference? Subjects were additionally asked whether they had fear or no fear. These questions were asked directly after injection, i.e. before subjects were able to see the injection, and also one day after the injections.

SAFETY, PK AND IMMUNOGENICITY OF I.D. AND S.C. ADALIMUMAB ADMINISTRATION

Adverse events were summarized by treatment group, in subsets of all treatment-emergent AEs, and separately for treatment-related AEs. Clinical laboratory and vital sign measurements were summarized by treatment and change from baseline was recorded. Summary statistics included number of subjects, mean, median, minimum and maximum values (with standard deviation). Immunogenicity, i.e. anti-adalimumab antibodies, was reported descriptively.

For PK analyses, serum adalimumab concentrations were assessed in blood collected in 4 mL plain tubes (BD) after coagulation (30–60 min) and centrifugation (2000 G for 10 min at 4°C), from day 1 (predose) to day 71 postdose. Adalimumab levels were quantified by fully automated enzyme-linked immunosorbent assay as described.[16] Briefly, TNF was indirectly coated on microtitre plates. Serum was added and incubated. Immobilized adalimumab was subsequently detected using biotinylated rabbit anti-idiotype. The lower limit of detection (LOD) for this assay is 10 ng/mL.

Anti-adalimumab antibodies were measured using a semi-quantitative radioimmunoassay as previously described.[16] Briefly, samples were incubated with sepharose-immobilized protein A (1.0 mg/TEST; Pharmacia Uppsala, Sweden) on its surface to capture IGG. After washing, radioactive-iodine labelled F(ab')2 fragments of adalimumab were added to detect drug-specific antibodies. The LOD for this assay 12 AU/mL.

Ex vivo whole blood challenge was performed to assess the effect of adalimumab on the release of cytokines by circulating immune cells and activation of these cells. Blood (6 mL) was collected in sodium heparin tubes (Becton Dickinson, NJ, USA) followed by stimulation with 2 ng/mL lipopolysaccharide (LPS; Sigma-Aldrich, Deisenhofen, Germany) and 25 µg/mL aluminium hydroxide (Alhydrogel 2%; Invivogen, Toulouse, France) for 24 hours at 37°C, 5% CO_2. Culture supernatants were assayed for release of proinflammatory cytokines TNFα, interleukin (IL)-6, IL-1β, IFNγ and IL-8 using the Mesoscale Discovery multiplex immunoassay platform.

USABILITY OF OPTICAL COHERENCE TOMOGRAPHY, CLINICAL PHOTOGRAPHY, THERMAL IMAGING AND LASER SPECKLE CONTRAST IMAGING IN THE EVALUATION OF I.D. INJECTIONS

Subjects were acclimatized in a temperature-controlled room (21°C) for 15 minutes with bare legs. The sequence of measurements was (starting with the least invasive to minimize disturbance of the subsequent measurements): (I) thermography; (II) cutaneous microcirculation; (III) 3D photography; (IV) multispectral imaging; and (v) skin morphology. Details of skin imaging methods are described below.

Skin microcirculation was quantified by LSCI (PeriCam PSI NR system, Perimed, Sweden). Laser speckle is the interference pattern returning from erythrocytes, resulting in a speckle pattern that differs under changes in blood flow.[17] Recordings of 40 seconds were taken from a distance of 15 cm with a reading frame of 7 × 7 cm. Analysis was performed using the internal software (PimSoft, Perimed, Sweden) and regions of interest were selected based on the most predominant injection site reaction. Area was calculated based on values above an arbitrary threshold of 90 PU.

Skin temperature was quantified by infrared thermography (FLIR X6540SC camera, FLIR Systems Inc., USA). After calibration for room temperature using a black body, 10 second recordings were taken from a distance of 80 cm. Recordings were averaged for analysis.

Skin morphology was assessed by OCT (D-OCT VivoSight, Michelson Diagnostics, UK). Thirty second scans were performed with a 6 mm diameter probe. Three automatically calculated parameters were used to quantify morphology (attenuation compensation, blood flow at depth and skin roughness). Qualitative analysis was performed by 2 clinical scientists with experience in analysing D-OCT images.

Erythema and swelling were quantified using a multispectral camera (Antera 3D, Miravex, Ireland), and a 3D stereophotogrammetry camera (3D LifeViz, QuantifiCare, USA). The multispectral camera was placed over the skin creating a closed environment with the lesion in the centre of the frame. Erythema was measured using the CIELab *a value. CIELab is a standardized quantitative method to discriminate colours using an XYZ-axis system. CIELab *a value is represented on the red/green axis (green colours are negative, red colours positive) and is correlated to skin erythema.[18,19] Three-dimensional images were taken from a distance of 20 cm with use of a guidance laser and analysed in imaging processing software (DermaPix Software, QuantifiCare, Valbonne, France). Volume was determined by outlining bleb circumference and height and calculated using the DermaPix (QuantifiCare, USA) algorithm for volume ($\sigma = 5$).

IN VITRO PROTEIN ANALYSIS

Adalimumab 100 mg/mL prefilled pens or syringes (depending on availability) of the same batch and expiration date were pooled. Storage containers were: (I) syringe only; (II) Verex 2 mL clear glass vial (Phenomenex, Torrance, CA, USA); and (III) syringe with a MicronJet600. For condition (I), a capped regular needle was attached during storage to prevent evaporation. Samples were measured immediately (to assess the effect of repackaging), or after storage for 4 hours at 4°C (to assess in-use stability). Directly before analysis the samples were ejected from the syringe into a glass vial and subsequently diluted to 10 or 1 mg/mL with solvent. The solvent consisted of Milli-Q water with 1.2 G per 100 mL mannitol (Sigma, St Louis, MO, USA) and 100 mg/100 mL polysorbate 80 (Sigma), and was filtered through an Anotop 10 mm, 0.1 µm syringe filter (Whatman, Maidstone, Kent, UK) before use. For nanoparticle tracking analysis (NTA) optimization, the solvent was made without polysorbate 80. Experiments were performed at room temperature, and in a dust free cabinet whenever possible. Changes in protein conformation were determined by second-derivative UV spectroscopy. The formation of adalimumab aggregates and particles was determined by dynamic light scattering (DLS), high-pressure size-exclusion chromatography (HP-SEC), micro-flow imaging (MFI) and NTA as described[20] and summarized below.

UV SPECTROSCOPY

Second-derivative UV spectroscopy was used to detect conformational changes. Measurements were performed on an Agilent 8453 UV–VIS spectrometer (Agilent Technologies, Waldbronn, Germany). Samples were measured in 2 mL half-micro quartz cuvettes (Hellma Benelux, Kruibeke, Belgium) with a path length of 10 mm in a concentration of 1 mg/mL. Absorbance was measured from 248 to 332 NM with 1 NM intervals and an integration time of 15 seconds. Background correction was performed using solvent. Second-derivative spectra were calculated with UV–Visible ChemStation software (Agilent Technologies, Walbronn, Germany) as described earlier.[20] The a/b ratio, i.e., the ratio between (I) the vertical distance between the peak minimum at 283 NM and the maximum at 287 NM and (II) the vertical distance between the minimum and maximum at 290 and 295 NM was calculated and used to determine the exposure of tyrosine residues to bulk solvent, which is sensitive to changes in the tertiary structure.[21]

DLS

DLS was used to detect aggregates in the size range from about 1 NM to 1 µm. DLS was performed on a Malvern Zetasizer Nano (Malvern, Herrenberg, Germany); 500 µL of each sample in a concentration of 10 mg/mL was analysed in plastic cuvettes at 25°C using the automatic mode (n = 3). Z-average diameter and polydispersity index were calculated using Dispersion Technology Software version 7.03 (Malvern, Herrenberg, Germany).

HP-SEC

HP-SEC was used to quantify monomers, dimers and fragments. Adalimumab samples of 1 mg/mL were injected in a volume of 50 µL onto a SRT SEC-300, 5 µm, 30 cm × 7.8 mm column (Supelco, Bellefonte, PA, USA). An Agilent 1200 chromatography system (Agilent Technologics, Palo Alto, California) combined with an Agilent 1200 UV detector and a multi-angle laser light scattering detector (DAWN HELEOS, Wyatt Technology Europe GmbH) was used. The flow rate was 0.5 mL/min. The mobile phase was composed of 50MM phosphate, 150MM arginine and 0.025% NaN_3 at pH 6.5. To quantify aggregation, UV absorption at 280 NM was recorded. From the multiangle laser light scattering signal, the root mean square diameter was calculated using the Berry Fit in the Astra software version 5.3.2.22 (Wyatt Technology Europe GmbH, Dernbach, Germany).

MFI

MFI was used to detect particles up to 70 µm. A MFI5200 (ProteinSimple, Santa Clara, AC, USA), equipped with a silane coated flow cell (1.41 × 1.76 × 0.1 mm) and controlled by the MFI View System Software version 2 was used. Prior to each

measurement the system was flushed with purified water. The background was zeroed by using solvent and performing the optimize illumination procedure. Samples of 1 mg/mL adalimumab were analysed without a predefined prerun volume because of the limited amount. Flow rate was 0.17 mL/min and camera shot rate was 22 flashes per second. Data were analysed with MFI View Analysis Suite version 1.2. For each product, stuck, edge, and slow-moving particles were removed by the software before analysis. Because no prerun volume could be used, the data were recorded throughout the entire run but processed only in the time window from 0.7 to 1.7 min where, based on the trend chart option in the software, the measurement was stable for all samples. The equivalent circular diameter was calculated as described earlier.[20]

NTA

NTA was used to detect particles between about 50 and 1000 NM. Measurements were performed with a NanoSight LM20, equipped with a sample chamber with a 635 NM laser for illumination of the particles. Samples of 10 mg/mL adalimumab were injected into the chamber by an automatic pump (Harvard Apparatus, catalogue no. 984362, Holliston, USA) using a sterile 1 mL syringe (BD Discardit II). For each sample, a 90 second video was captured with the shutter set at 29.9 ms and the gain at 680. Videos were analysed using NTA 2.0 Build 127 software. The following settings were used for tracking of the particles: background extract on; brightness 0; gain 1; blur size 3 × 3; detection threshold 10, viscosity 0.953. All other parameters were set to the automatic adjustment mode.

STATISTICS

The population analysed for pain, tolerability, preference, skin imaging and PD endpoints included all randomized subjects (n = 24 subjects). The population analysed for PK parameters and PK modelling included injections in which no spillage during treatment administration was reported (n = 43 injections). Repeated pain injection data (VAS and FPSR) were analysed with a repeated measures ANOVA with fixed factors treatment, method, time, treatment by method, treatment by time, method by time, treatment by method by time, random factor subject and repeated factor time within subject by treatment by method. The injection pain score of the Mantoux intradermal injection at screening was used as covariate. Single measured pain insertion data (VAS and FPSR) were analysed with a repeated-measures model ANOVA with fixed factors treatment, method, treatment by method, and repeated factor method within subject. The insertion pain score of the Mantoux intradermal injection at screening was used as covariate. Repeated cytokines data were analysed with a repeated-measures ANOVA with fixed factors method, time, method by time, repeated factor time within subject and the baseline as covariate. The contrasts of interest were s.c. vs. i.d. and s.c. vs. i.d. within compound. For imaging analyses, a subset of data was used as some variables were zero in some conditions or timepoints. If applicable, the factors of the mixed model were adjusted.

PK ANALYSES

PK parameters derived from serum sample concentrations were calculated using a noncompartmental analysis. The noncompartmental analysis was performed using R version 3.5.3[22] while the linear trapezoid rule was used for the calculation of areas under the plasma concentration–time curves (AUCs). Analysis of the differences between methods were based on least squares means from the ANOVA of the ln-transformed $AUC_{0\text{-}t}$,$AUC_{0\text{-}inf}$ and maximum plasma concentration (C_{max}). In addition, Wilcoxon tests were performed on time to reach C_{max} (T_{max}).

POPULATION PK MODELLING

The identification of structural differences in the PK properties of s.c. and i.d. administration, while accounting for covariates such as the presence of anti-adalimumab antibodies, was investigated using a population nonlinear mixed effects modelling approach in NONMEM (ICON plc, V7.3). Based on literature information, a 1-compartment structural model with linear absorption and linear elimination was used during model development.[23] For this structural model, the effect of anti-drug antibodies on the CL of adalimumab was tested as a time-varying covariate, increasing the CL of adalimumab at higher titre levels with the following equation: $CL = \emptyset TV_{CL} * (1 + \emptyset TV_{Titre\text{-}slope} * TITRE)$, Where individual TITRE levels proportionally increase the CL of an individual over time.

When a structural misspecification was identified in the absorption phase, modifications to the absorption part of the model were explored, in which transit models, different absorption compartments, and a model event time (MTIME) function in which the ka changes after an estimated time point, were investigated, modelled separately for each administration route.

After identification of the best structural absorption models for each route of administration, log-transformed interindividual variability was included following a forward inclusion procedure ($P < .01$) and covariates (age, weight, body mass index, gender, serum creatinine, and albumin) were explored following a forward-inclusion ($P < .01$) with backward-elimination ($P \leq .001$) procedure. Continuous covariates were tested following a power relationship centered around the median. Models were evaluated on basis of the objective function value, the parameter uncertainty (judged by the relative standard error), goodness-of-fit figures, individual model predictions vs. observations over time,

and confidence interval visual predictive checks based on 500 Monte Carlo simulations. Bootstrapping was not considered of added value as additional model evaluation tool. Data transformation was performed in R (V3.6.1[22]) and models were executed in conjunction with Perl-speaks-NONMEM (V4.8.1).[24]

STUDY APPROVAL

The study protocol was reviewed and approved by an independent medical ethics committee, the Medische Ethische Toetsingscommissie van de Stichting Beoordeling Ethiek Biomedisch Onderzoek (Assen, the Netherlands). All subjects provided informed consent prior to any study related procedures. The study was conducted at the Centre for Human Drug Research (Leiden, the Netherlands) from July 2018 until October 2018, and registered under clinical trial number NCT03607903. No interim analysis was performed.

RESULTS

Forty-seven subjects underwent medical screening. Twenty-four subjects (male:female ratio 1:1) with Fitzpatrick skin type II were administered 40 mg adalimumab (volume of 0.4 mL) i.d. or s.c. in the lateral upper thigh and placebo (volume of 0.4 mL) s.c. or i.d. in the contralateral thigh. One subject was randomized but excluded before treatment due to medical reasons and replaced (Figure 1). The mean age was 26.1 years (range 20–42). Demographic characteristics were comparable between groups (Table 1). For both s.c. and i.d. adalimumab injections, a minor spill (1–15% of intended volume not injected) occurred in 2 of 12 (17%) injections, and there was 1 (8%) major spill (15–50% of intended volume not injected) in an i.d. adalimumab injection. Both the minor spills and the major spill during i.d. injection occurred when high resistance during injection was encountered, whereas the minor spill of s.c. injection was due to backflow. Inspection of the hollow microneedles after injection using bright field microscopy did not show damaged microneedle tips (not shown).

Figure 1 CONSORT flow diagram of clinical trial. For pharmacokinetic and population pharmacokinetic analysis, subjects in whom any spillage occurred during injection were excluded. Other analyses were done with all subjects who completed the study (n = 24). i.d.: intradermal; s.c.: subcutaneous

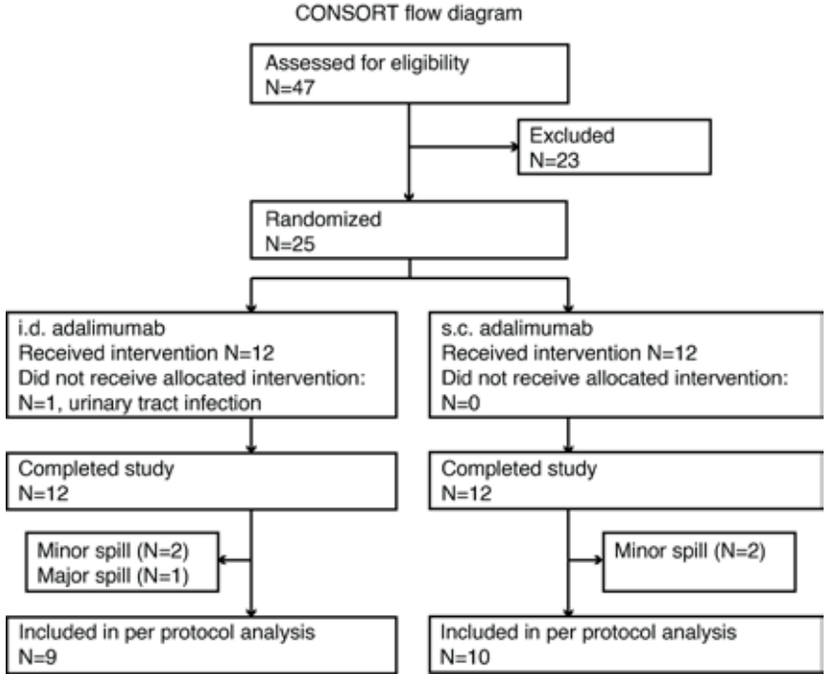

Table 1 Demographics and baseline characteristics

	All subjects n=24	
	i.d. (n=12)	s.c. (n=12)
Age (years)		
Mean (SD)	25.2 (5.3)	27.1 (7.6)
Median	23	23.5
Min-Max	20-38	20-42
Height (cm)		
Mean (SD)	177.8 (6.1)	180.1 (7.6)
Min-Max	167.3-188.5	166.5-191.1
BMI (kg/m²)		
Mean (SD)	23.8 (3.2)	23.2 (2.8)
Min-Max	19.3-29.3	20-28.8
Sex		
Female (%)	6 (25%)	6 (25%)
Male (%)	6 (25%)	6 (25%)
Race (% per group)		
Asian	0 (0%)	0 (0%)
Black or Afr. American	0 (0%)	0 (0%)
Mixed	0 (0%)	0 (0%)
Other	0 (0%)	0 (0%)
Caucasian	12 (100%)	12 (100%)

i.d.: intradermal; s.c.: subcutaneous; SD: standard deviation

PAIN, ACCEPTABILITY AND LOCAL TOLERABILITY AFTER I.D. AND S.C. ADALIMUMAB ADMINISTRATION

Pain ascribed to needle injections is often divided into insertion pain, which is pain resulting from the needle insertion, and injection pain which is pain resulting from the fluid injection. Insertion pain did not statistically significant differ between a hollow microneedle and a regular s.c. needle (Figure 2A, all p = .22). Pain associated with fluid injection was higher for i.d. vs. s.c. injections (Figure 2A, i.d. vs. s.c. estimated means 29.5 and 8.3, decrease of 72%, 95% confidence interval [CI] −83 to −53%, p < .001). Intradermal adalimumab injections were more painful (estimated mean 35.4) than s.c. adalimumab injections (estimated mean 7.9). Comparing the treatments (placebo vs. adalimumab, with both i.d. and s.c. administration methods combined) no statistically significant difference was observed (p = .55). There was no difference within the administration method between adalimumab or placebo administration (placebo vs. adalimumab within administration method p = .32 and p = .81 for i.d. and s.c., respectively). No pain was reported 24 hours after injection in any treatment group (Figure 2B). For both insertion and injection, a similar pattern in pain was reported in the Dutch FPSR15 in comparison with the VAS (data not shown). Altogether, these subject-reported outcomes indicate that there is no difference in pain between adalimumab and placebo injection, but that i.d. injection is more painful than s.c. injection.

Figure 2 Volunteer reported outcomes indicate preference for subcutaneous (s.c.) administration vs. intradermal (i.d.) administration. Healthy volunteers were injected with a single dose of adalimumab in the upper thigh and placebo in the contralateral upper thigh administered i.d. using a hollow microneedle or s.c. using a conventional needle. Insertion and injection pain were normalized to the pain score during a Mantoux which the volunteers received during screening. (A) Visual analogue scale (VAS) pain scores for insertion pain. No differences were observed between s.c. and i.d. insertion pain (p = .68). (B) VAS pain scores for injection and postinjection pain. Injection pain was significantly (p < .0001) higher for i.d. compared to s.c. injection. Postinjection pain was not present. After injection, subjects were asked multiple choice questions about their preference, for (C) how they experienced the injection, (D) how they would like to get a hypothetical future injection, (E) and for which injection they had fear. (A-E): n = 12 per group, except for Mantoux where n = 24. (A-B): mean ± standard deviation; repeated-measures ANOVA; **** P < .0001. NA: not available because not measured

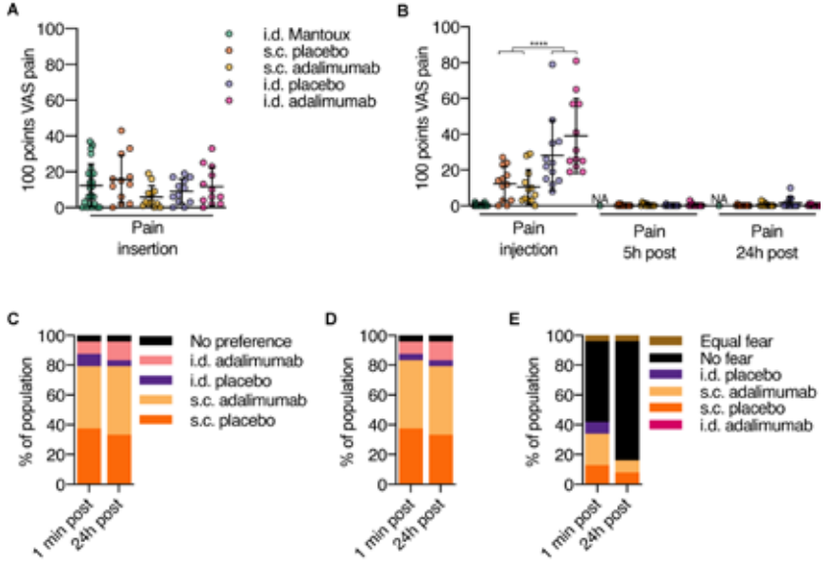

To determine which injection type was preferred, subjects were asked about their preference: immediately after the injections (i.e. before seeing the injection area) and also one day after the injections. Subject reported outcomes indicated that subjects had a preference for s.c. injection compared to i.d. injection (Figure 2C). They also preferred to receive a hypothetical next injection using s.c. rather than i.d. administration (Figure 2D). Directly after injection a majority (13 subjects, 54%) indicated no fear, while 24 hours after injection, most (19 subjects, 79%) subjects indicated no fear after injection. To summarize, we found that volunteers prefer s.c. over i.d. injection.

SAFETY

Nine treatment emergent adverse events were recorded; 5 in the s.c. group and 4 in the i.d. group. All treatment emergent adverse events were mild and self-limiting. Four subjects had fatigue, 3 had an upper respiratory tract infection, and 1 subject had a rhinitis. One subject had an injection site haematoma after i.d. adalimumab. Thus, i.d. and s.c. administration of adalimumab and saline do not raise a safety signal.

IMMUNOGENICITY

Anti-adalimumab antibodies are reported descriptively. None of the study participants had anti-adalimumab antibodies at baseline. Ten (83%, Figure 3A) and six (50%, Figure 3B) of the volunteers who received s.c. or i.d. adalimumab, respectively, treatment-emergent anti-adalimumab antibodies were detected. The median serum concentration for anti-adalimumab antibodies, for participants who developed anti-adalimumab antibodies, was 178 (range 16–864) for s.c. and 250 (range 189–940) arbitrary units for i.d. administration (Figure 3C). Presence of anti-adalimumab antibodies was associated with increased adalimumab CL. However, high variability in the $AUC_{0\text{-inf}}$ was identified due to the differences in immunogenicity, which needs to be taken into account to allow for a direct comparison of i.d. with s.c. administration.

PK OF I.D. AND S.C. ADALIMUMAB ADMINISTRATION

The adalimumab concentration time profile is displayed in Figure 3D. First, a noncompartmental analysis of PK was performed. After exclusion of subjects where any leakage occurred during injection, in the remaining subjects C_{max} was significantly higher after i.d. injection compared to s.c. injection (90% CI 0.57–0.90, p = .02). No difference was detected in $AUC_{0\text{-inf}}$ (90% CI 0.55–1.09, p = .22) or $AUC_{0\text{-last}}$ (90% CI 0.60–1.07, p = .20; per protocol subjects in Table 2, all enrolled subjects in Table S1). These data show that i.d. administration of adalimumab yields a higher maximum concentration than s.c. administered adalimumab.

Figure 3 Pharmacokinetics of adalimumab and anti-adalimumab antibodies after subcutaneous (s.c.) or intradermal (i.d.) injection. Mean anti-adalimumab levels after (A) s.c. and (B) i.d. administration (n = 12 per administration type). (C) Average anti-adalimumab levels for subjects with anti-adalimumab antibodies (n = 10 for s.c. administration and n = 6 for i.d. administration). (D) Serum adalimumab concentrations over time (D, n = 10 for s.c. administration and n = 9 for i.d. administration, noncompartmental analysis of subjects without leakage during injection). (C-D) Mean ± standard deviation. (E) Schematic depiction of population PK model. (F) Adalimumab absorption kinetics over time after adalimumab administration following microneedle i.d. or s.c. administration (typical population PK model). F: relative bioavailability; ka: absorption rate constant

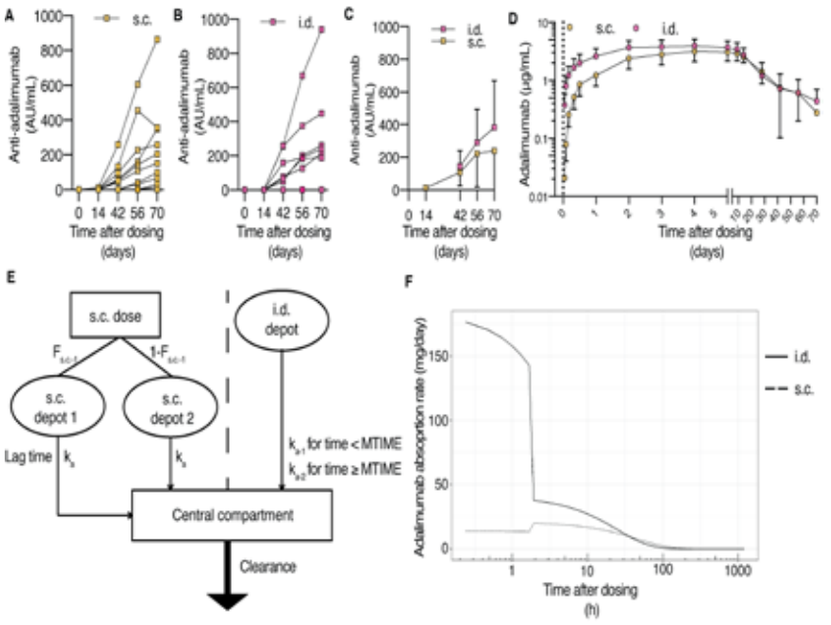

Table 2 Summary pharmacokinetic parameters for ID and SC adalimumab administration per protocol subjects, i.e. the subjects in which no leakage occurred and the intended dose of adalimumab was administered.

	s.c. (n=10)		i.d. (n=9)	
Parameter	**Mean (SD)**	**Median (range)**	**Mean (SD)**	**Median (range)**
C_{max} (µg/mL)	3.3 (1.1)	3.6 (1.5-4.8)	4.4 (0.7)	4.2 (3.6-5.5)
T_{max} (h)		120 (96-221)		95 (47-120)
$AUC_{0\text{-inf}}$ (µg*h/mL)	2359 (1167)	2048 (853-5351)	2986 (1217)	2724 (1679-4897)
$AUC_{0\text{-last}}$ (µg*h/mL)	2189 (816)	2005 (846-4019)	2688 (869)	2581 (1677-4094)

SD: standard deviation; C_{max}: maximum plasma concentration; T_{max}: time to reach C_{max}; AUC: area under the plasma concentration–time curve

To further examine PK and to be able to correct for interindividual variation in the kinetics of adalimumab and the formation of anti-adalimumab antibodies, a population PK model was developed. After exclusion of subjects in which any spill of adalimumab occurred during administration, data from 10 s.c. and 9 i.d. injections were available for model development using 275 adalimumab measurements that were above the LOD. A total of 4% of the measurements was below the LOD and therefore excluded from analysis. A significant effect between the time-varying titre levels and the CL was identified ($p < .001$), indicating that the CL of adalimumab increases in the presence of high titre levels. However, a bias in the absorption kinetics for s.c. and i.d. was identified with linear absorption kinetics. Subsequent exploration of different structural absorption models resulted in a MTIME function for the absorption rate constant (ka) after i.d. administration and 2 separate absorption compartments with equal kas and 1 with an absorption lag time for s.c. administration to be best fit for purpose (Figure 3E). In this revised structural model, significant ($p < .01$) interindividual variability on the titre-CL relationship and the central volume of distribution was identified. Additionally, a significant ($p < .01$) improvement in model fit was quantified after estimating a 29% higher relative bioavailability (F_{rel}) after i.d. administration of adalimumab compared to s.c. administered adalimumab. A negative age–CL relationship and a positive weight–CL relationship were identified. Both covariates gave $p < .001$ improvement in the model fit. The developed model showed an overall accurate description of the absorption and elimination phase of adalimumab (Figure S2). Model parameters (Table 3) were estimated with high precision and were comparable to literature values.[23] Simulations of the typical adalimumab absorption rates over time showed a clear difference between both administration routes, in which the i.d. dose had a fast initial phase which decreased after MTIME, whereas the s.c. administration had a slower initial phase and a small increase in the absorption rate, approximately 2 hours after dosing (Figure 3F).

Cytokine production was assessed by stimulating *ex vivo* whole blood with LPS and aluminium hydroxide, driving NF-κB and NLRP3 inflammasome activation. Results are shown in Figure 4. Free TNFα levels after both s.c. and i.d. administration sharply decreased from predose to postdose (mean levels predose i.d. 897 pg/mL, i.d. 48 h postdose 50 pg/mL, s.c. predose 928 pg/mL, s.c. 48 h postdose 74 pg/mL), as has been reported earlier,[16] and returned to baseline at the end of study (i.d. 70 d postdose 1149 pg/mL, s.c. 70 d postdose 850 pg/mL). No significant differences in inhibition of cytokine release were detected when i.d. adalimumab administration was compared to s.c. adalimumab administration (IFNγ $p = .61$; IL-6 $p = .31$; IL-8 $p = .81$; IL-1β $p = .61$; TNFα $p = .80$). A sex effect has been reported for LPS/aluminium hydroxide-induced IFNγ production after adalimumab administration,[14] but this was not detected in this study (IFNγ $p = .99$; IL-6 $p = .80$; IL-8 $p = .96$; IL-1β $p = .75$; TNFα $p = .08$).

Table 3 Population pharmacokinetics parameter estimates with relative standard errors.

Parameter	Estimate	RSE (%)
Absorption population parameters		
F_{ID}	1.29	6.46
Intradermal administration		
k_{a-1} (/day)	3.54	10.1
k_{a-2} (/day)	0.96	9.90
MTIME (days)	0.078	9.32
Subcutaneous administration		
k_a (/day)	0.514	9.64
F_{SC-1}	0.322	36.6
Lag time (days)	0.075	36.7
Structural model parameters		
Volume of distribution central (L)	11.5	8.02
Clearance (L/day)	0.36	4.31
Covariate relationships		
CL-age exponent[a]	-0.70	24.3
CL-weight exponent[b]	0.68	36.7
TITRE-slope (/xxx)	0.064	25.1
Inter-individual variability		
ω^2 Volume of distribution central	0.069	31.2
ω^2 TITRE-slope	0.537	37.1
Residual variability		
σ^2 Proportional residual error	0.054	13.9

CL: clearance; F: relative bioavailability; ka: absorption rate constant; MTIME, model event time; RSE: relative standard error / a) centred around 23 years / b) centred around 70 kg.

OPTICAL COHERENCE TOMOGRAPHY, CLINICAL PHOTOGRAPHY, THERMAL IMAGING AND LASER SPECKLE CONTRAST IMAGING

Three-dimensional photography was used to quantify the bleb size after i.d. injection. No bleb formation was observed after s.c. injection. After i.d. injection bleb formation was observed after both adalimumab and saline injections, which resolved in less than 1 day (Figure 5A,B). I.D. adalimumab administration but not s.c. adalimumab administration or injection of placebo caused local redness after injection (Figure 5C). OCT was used to examine breach of epidermis and fluid disposition. Penetration of the epidermis was visible for 92% of cases 10 minutes after administration of both placebo injections and s.c. adalimumab injection. All i.d. adalimumab injections showed epidermal penetration 10 minutes postdose (Figure 5D–F). Fluid disposition and vasodilatation in the dermis were visible more clearly for i.d. injections than s.c. injections.

Figure 4 Similar cytokine production after subcutaneous (s.c.) or intradermal (i.d.) adalimumab administration (A) tumour necrosis factor-α (TNFα), (B) interleukin (IL)-1β, (C) IL-8, (D) interferon (IFN)γ and (E) IL-6 release after *ex vivo* stimulation with lipopolysaccharide/aluminium hydroxide of whole blood samples. No sex effect was observed. Mean ± standard deviation. A-E: n = 12 per group, repeated measures ANOVA

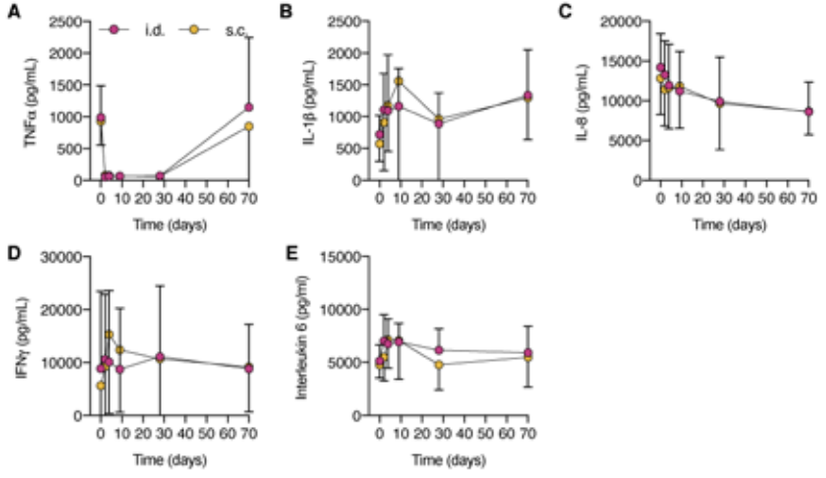

Cutaneous microcirculation of the upper legs following injections was quantified using LSCI. A significant increase in blood flow for i.d. adalimumab injections compared to i.d. placebo, s.c. adalimumab, and s.c. placebo injections was shown 10 minutes postdose ($p < .0001$, Figure 5G), followed by a decrease, reaching baseline on day 3 (data not shown). The bleb surface area was quantified using LSCI's perfused area measurements. The perfused areas were significant larger after i.d. adalimumab injections compared to i.d. placebo ($p < .0001$), and also compared to s.c. adalimumab ($p = .0012$) and placebo injections ($p < .0001$; Figure 5H,I).

Injection site temperature was measured in a temperature-controlled room using infrared thermography and corrected using standardized control areas (Figure S1).

IN VITRO PROTEIN ANALYSIS

In vitro studies were performed to investigate whether passage of adalimumab through a hollow microneedle led to protein instability, as compared to passage through a regular s.c. needle. To this end, adalimumab was subjected to the same storage conditions and ejection methods as those used in the clinical trial. Protein conformational changes were determined by second-derivative UV spectroscopy, and formation of adalimumab aggregates and particles were determined by DLS, HP-SEC, MFI and NTA. Results of the protein analysis are shown in Table 4. Second-derivative UV spectroscopy showed no change in a/b ratio between conditions and time points, indicating no protein conformational changes. With DLS, no substantial differences in Z-average diameter were found. No substantial differences in the concentration of particles ≥2 µm were detected between conditions using MFI. NTA showed nanoparticle concentrations around the lower limit of detection (10^7 ; data not shown), and mean sizes were found ranging from 188 to 414 NM. HP-SEC showed no differences in monomer content between conditions or between time points, and no evidence of aggregation or fragmentation. Molecular weights, based on multiangle laser light scattering data for the main peak, correspond to that of adalimumab reported before.[20] These data show that passage of adalimumab through a hollow microneedle before storage and after storage for 4 hours at 2–8°C does not lead to measurable protein aggregation or particle formation.

Table 4 Characterization of adalimumab after passage through a glass vial, a syringe, or a syringe with a hollow microneedle (SYR. + MN), at 0 hours and after storage at 4 °C for 4 hours. Representative data of 2 independent experiments.

	Time point	0h			4h		
	Condition	**Vial**	**Syr.**	**Syr. + MN**	**Vial**	**Syr.**	**Syr. + MN**
UV spectroscopy	a/b ratio	1.46	1.46	1.45	1.38	1.41	1.44
DLS	Z-average diameter	3.76	3.68	3.99	3.59	3.61	4.23
	in nm (SD)	(0.01)	(0.03)	(0.33)	(0.03)	(0.07)	(0.04)
	Polydispersity index	0.191	0.203	0.191	0.188	0.177	0.182
	(SD)	(0.003)	(0.039)	(0.002)	(0.001)	(0.080)	(0.009)
HP-SEC	Monomer content (%)	99.8	98.0	98.0	99.6	99.6	99.6
	Dimer content (%)	0.2	2.0	2.0	0.4	0.4	0.4
	Molecular weight monomer (10^5 Da)	1.57	1.50	1.53	1.55	1.55	1.55
NTA size estimation	Mean in nm (SD)	429 (233)	408 (180)	463 (330)	386 (182)	391 (234)	352 (179)
MFI	Particles ≥ 2 µm per mL	4581	4264	4033	3309	3631	4145

DLS: dynamic light scattering; SD: standard deviation; HP-SEC: high-pressure size-exclusion chromatography; NTA: nanoparticle tracking analysis; MFI: micro-flow imaging. UV spectroscopy, HP-SEC and MFI were measured with adalimumab samples diluted to 1 mg/mL, DLS and NTA in a concentration of 10 mg/mL.

Figure 5 Characterization of skin reaction following subcutaneous (s.c.) and intradermal (i.d.) injection. (A-C) 3D photography. (A) Typical bleb after i.d. injection. (B) Maximum height and volume of injection site. Bleb height and volume did not differ between i.d. adalimumab and i.d. placebo (height $p = .26$, volume $p = .29$). (D) Redness of the injection sites: The more positive the CIELAB *a ratio, the redder the injection site. I.D. adalimumab and placebo injections induced significantly more redness of the skin compared to s.c. adalimumab and placebo injections ($p < .0001$). Skin redness induced by adalimumab

injection was significantly higher for i.d. administration than for placebo injection ($p = .0014$; E, F) Representative OCT images of i.d. injection 10 minutes postinjection; (D, E) Cross-sectional planes of i.d. injection, and (F) top view of skin surface with 3 puncture holes. (G) Skin perfusion in arbitrary PU 10 minutes postinjection, measured with LSCI. (H) Injection site surface area 10 minutes postinjection. A significant difference in skin perfusion and surface area 10 minutes postinjection was observed for both administration methods ($p < .0001$) and treatment ($p < .0001$). (I) Representative LSCI images of both injection methods and treatments 10 minutes postinjection. LSCI: laser speckle contrast imaging; OCT: optical coherence tomography; PU: perfusion units; B, D, G, H: mean ± standard deviation, n = 12 per group, repeated measures ANOVA, **** $p < .0001$

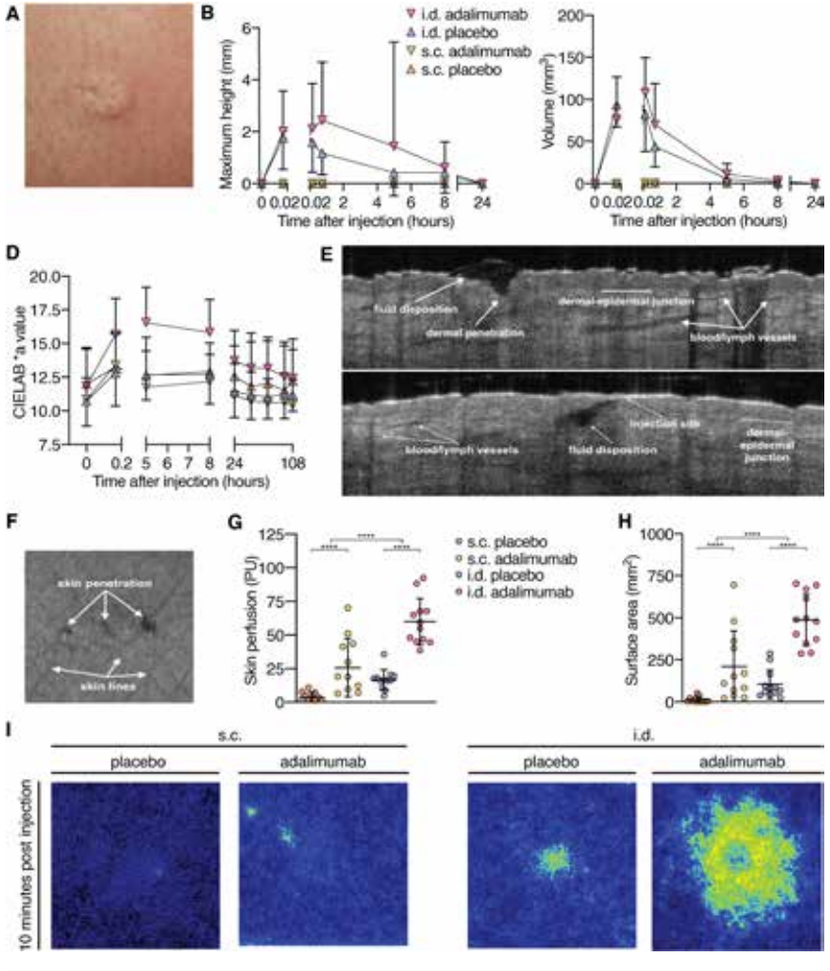

DISCUSSION

With a sophisticated and comprehensive, multimodal PK-PD safety approach we investigated a possibly minimally invasive administration method of adalimumab with a commercially available hollow microneedle. Importantly, this clinical trial shows that i.d. administration of a single dose of 40 mg adalimumab in a volume of 0.4 mL using a hollow microneedle is safe and well accepted. However, i.d. administration was associated with an increased amount of injection pain and decreased volunteer preference compared to s.c. administration. Using imaging methods, the effect of i.d. injections on the skin was thoroughly characterized. As expected, i.d. injections led to bleb formation. Notably, i.d. injection transiently increased cutaneous microcirculation as measured by LSCI. Importantly, we found that i.d. administration of adalimumab led to a higher C_{max} and a higher relative bioavailability compared to s.c. adalimumab administration. The inhibition of *ex vivo* cytokine production of whole blood stimulated with LPS/aluminium hydroxide was similar for i.d. and s.c. adalimumab administration indicating comparable PD efficacy.

Protein degradation, especially aggregation, might result in increased immunogenicity of mAbs[11] and immunogenicity of mAbs is a major reason for secondary loss of response to mAbs. Therefore, we first showed in vitro that microneedle ejection of adalimumab does not substantially alters the amount of protein fragments or aggregates compared to ejection using a regular hypodermic needle.

Hollow microneedles are frequently considered a minimally invasive device to deliver parenteral drugs.[4,25,26,27] In this study, we administered a single adalimumab dose of 40 mg in 0.4 mL or 0.4 mL placebo. We systematically studied pain associated with insertion and injection in a double-blind manner. We found that insertion pain of s.c. and i.d. administration was equal. However, injection pain of i.d. administration was significantly higher than s.c. administration. The high amount of pain is in contrast with another study, which used higher volumes but detected less pain.[27] Pain due to s.c. injection is generally attributed to different factors, i.e. volume of injection, site of injection, formulation, needle size and injection depth.[28]

The volume limit of s.c. injection is generally considered to be 1.5 mL.[29] Several studies have found higher volumes of s.c. administration to be associated with more pain.[29,30,31] Thus, the increased pain that was associated with i.d. administration in the clinical trial reported in this paper is probably due to the volume injected. The volume used in this trial was limited by a minimum volume which contains a regular dose of a MAB in adults. Future studies might investigate the volume-pain relationship for i.d. administration using hollow microneedles. We

did not detect a significant difference in pain when comparing adalimumab with placebo after i.d. and s.c. administration, which indicates that the formulation chosen in this study did not influence pain.

Although not quantified, we observed a higher injection pressure during i.d. administration compared to s.c. administration. With OCT, we detected fluid filled cavities after i.d. injection, indicating that there was no time for the compound to distribute in the skin.

We characterized the skin response to hollow microneedle administration of adalimumab using a combination of methods. The skin response following i.d. administration of adalimumab was mild and resolved within a day after injection. Using 3D photography, we showed a bleb, which is typical for i.d. administration. Furthermore, using LSCI, an increase in cutaneous microcirculation after i.d. injection of adalimumab was observed. Our observations are of interest in the context of drug absorption. The increased cutaneous microcirculation might be associated with the increased adalimumab absorption following i.d. vs. s.c. administration observed in our study. However, drugs injected s.c. may be absorbed via the lymph capillaries, or diffuse into blood capillaries, and after s.c. administration proteins with a high molecular weight, such as mAbs, are predominantly absorbed via the lymph after s.c. administration.[32,33]

Various factors influence lymph flow, one being local skin temperature. During an increase in local skin temperature, both the blood flow and the lymph flow increase.[34,35,36] We quantified local skin temperature after i.d. adalimumab administration using thermography. A limitation is that from the skin temperature measurements we cannot unequivocally conclude which type of injection (s.c. or i.d.) leads to higher skin temperature for two reasons. The temperature measurements might be confounded by difference in depth as i.d. injections are more superficial than s.c. injections. Thus, the s.c. injections might have increased the local temperature, which is not apparent from our measurements.

Initial lymphatics, the part of the lymph vessels responsible for drug uptake, are located superficially, in the dermis.[37] Under physiological conditions most of these lymph vessels are collapsed. Excess fluid (high hydrostatic pressure) and proteins (high local osmotic pressure) in the dermis cause high lymph flow. We used OCT to visualize epidermal penetration after i.d. injection. Qualitative analysis of OCT observations showed an increase in vessel diameter after i.d. injection compared to s.c. injection. Based on the OCT, no distinction can be made between blood and lymph vessels. Perhaps in the future, a new variant of OCT, Doppler OCT,[38] could be used to further characterize the physiology of MAB absorption and lymph flow.

Several studies have reported that the i.d. administration of drugs has different PK characteristics from s.c. delivery.[5,7,27,39] General observations are that T_{max} is decreased, C_{max} is increased and that relative bioavailability is either equal or increased after i.d. administration compared to s.c. administration. Most studies use insulin as model drug. For i.d. injection of insulin using hollow microneedles, it has been reported that C_{max} increases and T_{max} decreases after i.d. administration VS. s.c. administration. It has been suggested that a shift in the concentration–time profile explains why some but not all studies have reported increased relative bioavailability after i.d. injection.[5,40] Changes in PK are generally attributed to anatomical differences in the skin: the dermis has extensive vasculature and lymphatics, while the subcutis has more adipose tissue.[41] When correcting for individual differences in the covariates and the titre values, this study showed a significant difference in relative bioavailability between s.c. and i.d. administration; i.d. administration was associated with a 29% higher relative bioavailability. In our study, a clear distinction in the absorption profiles over time could be observed between s.c. and i.d. administration. Adalimumab administered by microneedle injection show a short but fast absorption, whereas s.c. dosing shows a lower absorption rate. The steep drop in absorption after a microneedle injection is caused by the distribution of sampling points and an estimated mathematical time point. In reality, this transition would probably be smoother. Altogether, the PK profile of the i.d. administration of adalimumab is favourable over s.c. administration.

The immunogenicity of mAbs is a significant clinical problem hampering the treatment of autoimmune diseases with mAbs. In this study, the number of healthy volunteers allows only for descriptive reporting of anti-adalimumab antibodies. The skin is a potent immune organ.[41] Studies have shown an increased immunogenicity of i.d. vaccines compared to s.c. vaccines and microneedles are frequently studied as a device to deliver vaccines.[42,43] By contrast, it has been suggested that i.d. administration of mAbs might lead to less immunogenicity compared to s.c. administration due to the presence of professional antigen-presenting cells in the epidermis and dermis rather than in the subcutis.[32,44] Perhaps the relatively short residence time at the i.d. injection site of the (predominantly monomeric) protein might contribute to the lack of increased immunogenicity as compared to s.c. administration. It remains to be determined whether i.d. administration of biologicals alters the incidence, degree, or time of onset of anti-drug antibody formation compared to s.c. administration.

In this study the functional effect of adalimumab administration was investigated in vitro. Whole blood was stimulated with LPS/aluminium hydroxide and secreted cytokines were measured. We found that i.d. and s.c. adalimumab reduced *ex vivo* TNFα bioavailability to a similar extent.

The increased relative bioavailability of i.d. adalimumab in our study suggests that lower doses may be used to achieve similar concentrations and subsequent

effects compared to s.c. administration. Combined with the increased elasticity of the skin of children[45] and the need for a lower (adalimumab) dose than in adults, hollow microneedles ultimately might be suitable for use in pediatric patients. However, it is of paramount importance to better understand the pain–volume relationship of i.d. injections using hollow microneedles in adults first.

In conclusion, we showed that the i.d. administration of adalimumab is feasible and leads to faster absorption and increased relative bioavailability compared to s.c. administration. The amount of pain reported in this study, higher for i.d. than for s.c. adalimumab administration, is probably explained by the injection volume of 0.4 mL. Understanding the relationship between pain and the administration of mAbs is essential before hollow microneedles can be investigated for use in the pediatric patient population.

ACKNOWLEDGEMENTS

We are indebted to our volunteers, and thankful to the team at the Centre for Human Drug Research and the pharmacy of the Leiden University Medical Center. Thanks to Karen Broekhuizen, medical writer at the Centre for Human Drug Research, who edited the manuscript for clarity. Funding: Dutch Arthritis Foundation: BP15–1-262.

REFERENCES

1 Nelson AL, Dhimolea E, Reichert JM. Development trends for human monoclonal antibody therapeutics. Nat Rev Drug Discov. 2010;9(10):767-774.
2 Jacobse J, Ten Voorde W, Rissmann R, Burggraaf J, Ten Cate R, Schrier L. The effect of repeated methotrexate injections on the quality of life of children with rheumatic diseases. Eur J Pediatr. 2019;178(1):17-20.
3 Donnelly RF, Raghu Raj Singh T, Larraneta E, McCrudden MTC. Microneedles for Drug and Vaccine Delivery and Patient Monitoring. Chichester, UK: John Wiley & Sons, Ltd; 2018.
4 Gupta J, Felner EI, Prausnitz MR. Rapid Pharmacokinetics of Intradermal Insulin Administered Using Microneedles in Type 1 Diabetes Subjects. Diabetes Technol Ther. 2011;13(4):451-456.
5 McVey E, Hirsch L, Sutter DE, et al. Pharmacokinetics and postprandial glycemic excursions following insulin lispro delivered by intradermal microneedle or subcutaneous infusion. J Diabetes Sci Technol. 2012;6(4):743-754.
6 Kochba E, Levin Y, Raz I, Cahn A. Improved Insulin Pharmacokinetics Using a Novel Microneedle Device for Intradermal Delivery in Patients with Type 2 Diabetes. Diabetes Technol Ther. 2016;18(9):525-531.
7 Milewski M, Manser K, Nissley BP, Mitra A. Analysis of the absorption kinetics of macromolecules following intradermal and subcutaneous administration. Eur J Pharm Biopharm. 2015;89:134-144.
8 Hróbjartsson A, Emanuelsson F, Thomsen ASS, Hilden J, Brorson S. Bias due to lack of patient blinding in clinical trials. A systematic review of trials randomizing patients to blind and nonblind sub-studies. Int J Epidemiology. 2014;43(4):1272-1283.
9 Levin Y, Kochba E, Kenney R. Clinical evaluation of a novel microneedle device for intradermal delivery of an influenza vaccine: Are all delivery methods the same? Vaccine. 2014;32(34):4249-4252.
10 Mahler SM, Marquis CP, Brown G, Roberts A, Hoogenboom HR. Cloning and expression of human V-genes derived from phage display libraries as fully assembled human anti-TNFα monoclonal antibodies. Immunotechnology. 1997;3(1):31-43.
11 Hermeling S, Crommelin DJA, Schellekens H, Jiskoot W. Structure-immunogenicity relationships of therapeutic proteins. Pharm Res. 2004;21(6):897-903.
12 Bartelds GM, Wijbrandts CA, Nurmohamed MT, et al. Clinical response to adalimumab: Relationship to anti-adalimumab antibodies and serum adalimumab concentrations in rheumatoid arthritis. Ann Rheum Dis. 2007;66(7):921-926.
13 Bartelds GM, Krieckaert CLM, Nurmohamed MT, et al. Development of Antidrug Antibodies Against Adalimumab and Association With Disease Activity and Treatment Failure During Long-term Follow-up. JAMA. 2011;305(14):1460-1468.
14 Dillingh MR, Reijers JAA, Malone KE, et al. Clinical evaluation of humira® biosimilar ons-3010 in healthy volunteers: Focus on pharmacokinetics and pharmacodynamics. Front Immunol. 2016;7:508.
15 Hicks CL, Von Baeyer CL, Spafford PA, Van Korlaar I, Goodenough B. The Faces Pain Scale - Revised: Toward a common metric in pediatric pain measurement. Pain. 2001;93(2):173-183.
16 Pouw MF, Krieckaert CL, Nurmohamed MT, et al. Key findings towards optimising adalimumab treatment: The concentration-effect curve. Ann Rheum Dis. 2015;74(3):513-518.
17 Briers D, Duncan DD, Hirst E, et al. Laser speckle contrast imaging: theoretical and practical limitations. J Biomed Opt. 2013;18(6):066018.
18 Everett JS, Budescu M, Sommers MS. Making Sense of Skin Color in Clinical Care. Clin Nurs Res. 2012;21(4):495-516.
19 Del Bino S, Bernerd F. Variations in skin colour and the biological consequences of ultraviolet radiation exposure. Br J Dermatol. 2013;169(SUPPL. 3):33-40.
20 Vlieland ND, Nejadnik MR, Gardarsdottir H, et al. The Impact of Inadequate Temperature Storage Conditions on Aggregate and Particle Formation in Drugs Containing Tumor Necrosis Factor-Alpha Inhibitors. Pharm Res. 2018;35(2):42.
21 Kueltzo LA, Middaugh CR. Ultravioloet absorption spectroscopy. In: Jiskoot W, Crommelin DJA, eds. Methods for structural analysis of protein pharmaceuticals. Arlington: AAPS Press; 2005.
22 R Core Team . (2017). R: A language and environment for statistical computing. R Foundation for Statistical Computing, Vienna, Austria. URL: https://www.R-project.org/
23 Berends SE, Strik AS, Van Selm JC, et al. Explaining Interpatient Variability in Adalimumab Pharmacokinetics in Patients with Crohn's Disease. Ther Drug Monit. 2018;40(2):202-211.
24 Lindbom L, Ribbing J, Jonsson EN. Perl-speaks-NONMEM (PsN) - A Perl module for NONMEM related programming. Comput Methods Programs Biomed. 2004;75(2):85-94.
25 Kim YC, Park JH, Prausnitz MR. Microneedles for drug and vaccine delivery. Adv Drug Deliv Rev. 2012;64(14):1547-1568.
26 Gill HS, Denson DD, Burris BA, Prausnitz MR. Effect of microneedle design on pain in human volunteers. Clin J Pain. 2008;24(7):585-594.
27 Gupta J, Park SS, Bondy B, Felner EI, Prausnitz MR. Infusion pressure and pain during microneedle injection into skin of human subjects. Biomaterials. 2011;32(28):6823-6831.
28 28. Usach I, Martinez R, Festini T, Peris JE. Subcutaneous Injection of Drugs: Literature Review of Factors Influencing Pain Sensation at the Injection Site. Adv Ther. 2019;36(11):2986-2996.
29 29. Mathaes R, Koulov A, Joerg S, Mahler HC. Subcutaneous Injection Volume of Biopharmaceuticals—Pushing the Boundaries. J Pharm Sci. 2016;105(8):2255-2259.
30 30. Heise T, Nosek L, Dellweg S, et al. Impact of injection speed and volume on perceived pain during subcutaneous injections into the abdomen and thigh:

a single-centre, randomized controlled trial. Diabetes Obes Metab. 2014;16(10):971-976.
31 31. Jørgensen JT, Rømsing J, Rasmussen M, Møller-Sonnergaard J, Vang L, Musæus L. Pain assessment of subcutaneous injections. Ann Pharmacother. 1996;30(7–8):729-732.
32 32. Richter WF, Bhansali SG, Morris ME. Mechanistic determinants of biotherapeutics absorption following SC administration. AAPS J. 2012;14(3):559-570.
33 33. Supersaxo A, Hein WR, Steffen H. Effect of molecular weight on the lymphatic absorption of water-soluble compounds following subcutaneous administration. Pharm Res. 1990;7(2):167-169.
34 34. O'Morchoe CCC, Jones WR, Jarosz HM. Temperature dependence of protein transport across lymphatic endothelium in vitro. J Cell Biol. 1984;98(2):629-640.
35 35. Astrup A, Bülow J, Madsen J. Skin temperature and subcutaneous adipose blood flow in man. Scand J Clin Lab Invest. 1980;40(2):135-138.
36 36. Olszewski W, Engeset A, Icger PM, Sokolowski J, Theodorsen L. Flow and Composition of Leg Lymph in Normal Men during Venous Stasis, Muscular Activity and Local Hyperthermia. Acta Physiol Scand. 1977;99(2):149-155.
37 37. Ryan TJ, Mortimer PS, Jones RL. Lymphatics of the Skin: Neglected but Important. Int J Dermatol. 1986;25(7):411-419.
38 38. Blatter C, Meijer EFJ, Nam AS, et al. *In vivo* label-free measurement of lymph flow velocity and volumetric flow rates using Doppler optical coherence tomography. Sci Rep. 2016;6:29035.
39 39. Dul M, Stefanidou M, Porta P, et al. Hydrodynamic gene delivery in human skin using a hollow microneedle device. J Control Release. 2017;265:120-131.
40 40. Rini CJ, McVey E, Sutter D, et al. Intradermal insulin infusion achieves faster insulin action than subcutaneous infusion for 3-day wear. Drug Deliv Transl Res. 2015;5(4):332-345.
41 41. Kabashima K, Honda T, Ginhoux F, Egawa G. The immunological anatomy of the skin. Nat Rev Immunol. 2019;19(1):19-30.
42 42. Lambert PH, Laurent PE. Intradermal vaccine delivery: Will new delivery systems transform vaccine administration? Vaccine. 2008;26(26):3197-3208.
43 43. Prausnitz MR, Mikszta JA, Cormier M, Andrianov AK. Microneedle-Based Vaccines. Curr Top Microbiol Immunol. 2009;333:369-393.
44 44. Büttel IC, Chamberlain P, Chowers Y, et al. Taking immunogenicity assessment of therapeutic proteins to the next level. Biologicals. 2011;39(2):100-109.
45 45. Rittié L, Fisher GJ. Natural and sun-induced aging of human skin. Cold Spring Harb Perspect Med. 2015;5(1):1-14.
46 46. Alexander SPH, Kelly E, Mathie A, et al. The Concise Guide to pharmacology 2019/20. Br J Pharmacol. 2019;176(S1) I-IV and:S1-S493.

Supplementary Table 1 Summary pharmacokinetic parameters for i.d. (A) and s.c.(B) adalimumab administration for all enrolled subjects.

A

	s.c. (n=12)		i.d. (n=12)	
Parameter	**Mean (SD)**	**Median (range)**	**Mean (SD)**	**Median (range)**
C_{max} (mug/mL)	3.3 (1.0)	3.4 (1.5-4.8)	4.0 (4.1)	4.1 (1.6-5.6)
T_{max} (h)	145 (54)	120 (96-221)	90 (23)	96 (47-120)
$AUC_{0\text{-}inf}$ (µg*h/mL)	2401 (1094)	2054 (853-5316)	2514 (1173)	2623 (619-4805)
$AUC_{0\text{-}last}$ (µg*h/mL)	2130 (690)	2005 (846-2603)	2332 (976)	2485 (619-4805)
CL (L/h)	0.02 (0.01)	0.02 (0.01-0.05)	0.02 (0.02)	0.02 (0.01-0.06)

B

	s.c. (n=10)		i.d. (n=9)	
Parameter	**Mean (SD)**	**Median (range)**	**Mean (SD)**	**Median (range)**
C_{max} (mug/mL)	3.3 (1.1)	3.6 (1.5-4.8)	4.4 (0.7)	4.2 (3.6-5.5)
T_{max} (h)	142 (120)	120 (96-221)	85 (85)	95 (47-120)
$AUC_{0\text{-}inf}$ (µg*h/mL)	2359 (1167)	2048 (853-5351)	2986 (1217)	2724 (1679-4897)
$AUC_{0\text{-}last}$ (µg*h/mL)	2180 (816)	2005 (846-4019)	2688 (869)	2581 (1677-4094)
CL (L/h)	0.02 (0.01)	0.02 (0.01-0.05)	0.02 (0.01	0.01 (0.01-0.02)

Supplementary Figure 1 Skin temperature after s.c. and i.d. injections. (A) Control thermography recordings were subtracted from injection site temperatures to calculate the difference in °C as change from baseline on a time point for the first day after injection. n = 12 per group, mean ± SD. (B) Images in the top panel are representative of reactions 1 minute postdose, and images in the bottom panel are representative of reactions 10 minutes postdose.

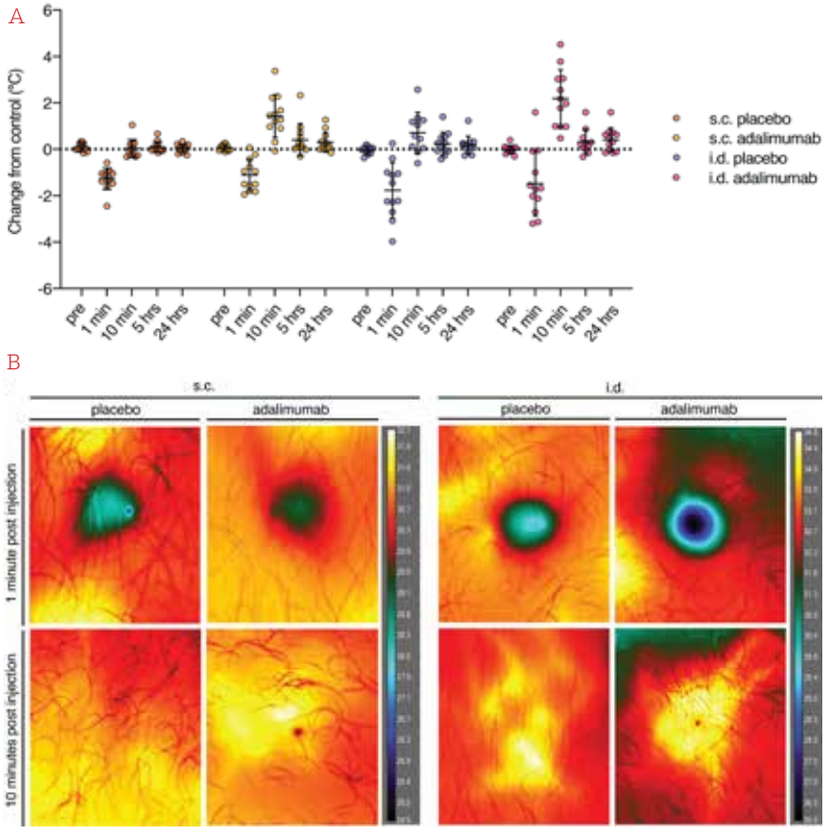

Supplementary Figure 2 Model fit of population PK model 500 Monte Carlo simulations were performed for a visual predictive check of the adalimumab population PK model after the development of a separate structural model for the absorption of microneedle (A) and s.c. (B) administration of adalimumab. The blue coloured rectangles are the 95% confidence interval around the 5 and 95% prediction interval. The orange rectangles are the 95% confidence interval around the median prediction. Data was binned per observation time. The dashed lines are the 5, 50 and 95% distribution of the data.